Magnetohydrodynamic and radiation effects on stagnation-point flow of nanofluid towards a nonlinear stretching sheet

M I Anwar[1], S Sharidan[1,]*, I Khan[1] & M Z Salleh[2]

[1]Department of Mathematical Sciences, Faculty of Science, Universiti Teknologi Malaysia (UTM) 81310 Skudai, Johor, Malaysia

[2]Faculty of Industrial Science and Technology, Universiti Malaysia Pahang (UMP) 26300 Kuantan, Pahang, Malaysia

Magnetohydrodynamic and radiation effects on stagnation-point flow of nanofluid towards a nonlinear stretching sheet under the assumption of a small magnetic Reynolds number have been studied. Sheet is stretched with a power law velocity in the presence of a non-uniform magnetic field $B(x)$ applied in a transverse direction. A nonlinear problem is modelled using the modified Bernoulli's equation for an electrically conducting fluid. Appropriate similarity transformations are used to reduce the governing nonlinear partial differential equations into a system of ordinary differential equations. These equations subjected to the boundary conditions are solved numerically by using the Keller-box method. Numerical results are plotted and discussed for pertinent flow parameters. A comparison with previous results in literature is also provided. The boundary layers are found shortened when free stream velocity is greater than stretching velocity.

Keywords: Magnetohydrodynamic flow, Nanofluid, Nonlinear stretching sheet, Radiation effect, Stagnation-point flow

Nanofluid studies have become an extensive area of research due to their growing applications in many industrial, engineering and technological processes such as chemical catalytic reactors, grain storage installations, diffusion of medicine in blood veins and cooling of electronic equipment. A limited attention was given to these fluids because of the additional nonlinear terms in the equation of motion that makes it more complex. There are some important studies for some intricate viscous fluid models introduced in the literature[1-3] and for nanofluid some recent studies have been conducted[4-6]. Choi[7] introduced convection heat transfer fluids as nanofluid having substantially higher thermal conductivities to study the enhancement in heat transfer phenomenon. Furthermore, some important experimental studies have been done[8-10] to evaluate the increase in the thermal conductivities of nanofluid.

On the other hand, a stagnation-point occurs whenever a flow impinges on a solid object. For orthogonally or non-orthogonally/obliquely stagnated flows, the velocities go to zero along with the highest pressure on the surface[11]. Based on the pioneering work of Heimenz[12] many researchers have discussed the stagnation point flows on stretching sheet[13-15].

Mustafa et al.[16] studied the stagnation point flow of a nanofluid towards a stretching sheet. Hamad and Ferdows[17] presented a Lie group analysis to find the similarity solution of boundary layer stagnation-point flow towards a heated porous stretching sheet saturated with a nanofluid with heat absorption/ generation and suction/blowing. After words, Alsaedi et al.[18] obtained results for convective boundaries by considering the effects of heat generation/absorption on stagnation-point flow. Recently, Nadeem et al.[19] reported solutions for axi-symmetric stagnation flow of a micropolar nanofluid in a moving cylinder.

In addition, the study of MHD stagnation-point flow over a nonlinearly stretching sheet has important applications in several manufacturing processes from industry such as extrusion of polymers, the cooling of metallic plates and aerodynamic extrusion of plastic sheet[20]. Having such a motivation, Hayat et al.[21] studied MHD flow of a micropolar fluid near a stagnation-point towards a nonlinear stretching surface. Mahapatra and Gupta[22] considered the MHD stagnation-point flow towards a stretching sheet. However, such studies for nanofluid are found to be scanty. To the best of our knowledge, no attention has been focused on MHD and radiation effects on stagnation-point flow of nanofluid towards a nonlinear stretching sheet. Hence, in the present paper, this study has been reported.

_____
*Corresponding author.
E-mail: ridafie@yahoo.com

Experimental Methodology

The unsteady two dimensional boundary layer stagnation-point flow of a nanofluid over a nonlinear stretching sheet is considered. The stretching and free stream velocities are assumed to be of the forms $u_w(x) = ax^m$ and $u_\infty(x) = bx^m$ respectively, where a and b are constants, $m\ (m \geq 0)$ is the velocity exponent parameter[23] and x is the coordinate measured along the stretching surface. A non-uniform transverse magnetic field of strength $B(x)$ is imposed in the $y-$direction normal to the flat sheet. It is assumed that the induced magnetic field due to the motion of the electrically conducting nanofluid is negligible. Further, it is also assumed that the external electrical field is zero and the electric field due to the polarization of charges is negligible. It is assumed that at the stretching surface, the temperature T and the nanoparticles fraction C take constant values T_w and C_w whereas the ambient values of temperature T_∞ and the nanoparticles fraction C_∞ are attained as y tends to infinity (Fig. 1). The governing boundary layer equations that are based on the balance laws of mass, linear momentum, energy and concentration species for the present problem [4, 16, 20] are given below:

$$\nabla.\text{V} = 0 \qquad\qquad\qquad\qquad\qquad \dots(1)$$

$$_f\left(\frac{\partial \text{V}}{\partial t} + (\text{V}.\nabla)\text{V}\right) = -\nabla p + \ \nabla^2 \text{V} - \ \text{B}^2(x)\text{V} \qquad \dots (2)$$

$$(\ c)_f\left(\frac{\partial T}{\partial t} + \text{V}.\nabla T\right) = k\nabla^2 T - \frac{1}{(\ c)_f}\nabla\cdot\mathbf{q}_r + (\ c)_p\left[D_B\nabla C.\nabla T + \left(\frac{D_T}{T_\infty}\right)\nabla T.\nabla T\right]$$
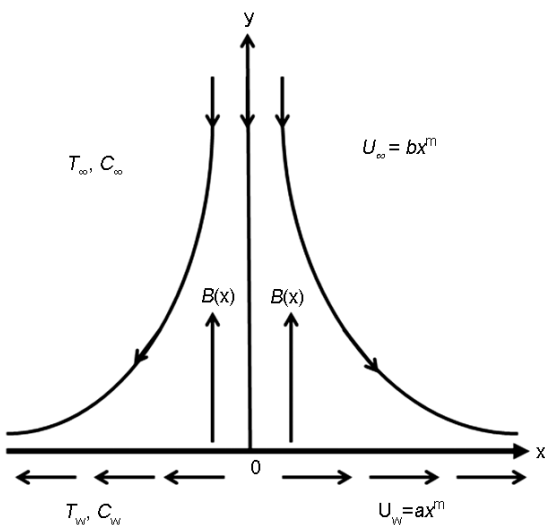$$\dots(3)$$

Fig. 1–Physical model and coordinate system

$$\frac{\partial C}{\partial t} + \text{V}.\nabla C = \text{D}_\text{B}\nabla C + \left(\frac{\text{D}_\text{T}}{\text{T}_\infty}\right)\nabla^2\text{T} \qquad \dots (4)$$

where V is the velocity vector;   , the electrical conductivity; B, the magnetic field; , the viscosity; $_f$, the density of the base fluid; D_B, the Brownian diffusion coefficient; D_T, the thermophoresis diffusion coefficient; k the thermal conductivity; $(\ c)_p$, the heat capacitance of the nanoparticles; $(\ c)_f$, the heat capacitance of the base fluid and q_r, the Rosseland approximation as defined[24, 25] below:

$$q_\text{r} = -\frac{4\ ^*}{3\text{k}^*}\left[\frac{\partial \text{T}^4}{\partial x}, \frac{\partial \text{T}^4}{\partial y}, \frac{\partial \text{T}^4}{\partial z}\right] \qquad \dots (5)$$

where * is the Stefan-Boltzmann constant; and k^*, the mean absorption coefficient. It is assumed that the temperature difference between the free stream temperature T_∞ and local temperature T is small enough, expanding T^4 in a Taylor series about T_∞ and neglecting higher order terms results for

$$T^4 \cong 4T_\infty^3 T - 3T_\infty^4 \qquad \dots (6)$$

For the steady laminar two-dimensional stagnation-point flow, Eqs (1)-(4) respectively reduce to

$$\frac{\partial u}{\partial x} + \frac{\partial v}{\partial y} = 0 \qquad\qquad\qquad \dots(7)$$

$$\frac{\partial p}{\partial x} = \ \frac{\partial^2 u}{\partial y^2} - \ _f\left(u\frac{\partial u}{\partial x} + v\frac{\partial u}{\partial y}\right) - \ \text{B}^2(x)u \qquad \dots(8)$$

$$u\frac{\partial T}{\partial x} + v\frac{\partial T}{\partial y} = \left(\ + \frac{16\ ^*T_\infty^3}{3k^*(\ c)_f}\right)\frac{\partial^2 T}{\partial y^2} + \left[D_B\frac{\partial C}{\partial y}\frac{\partial T}{\partial y} + \frac{D_T}{T_\infty}\left(\frac{\partial T}{\partial y}\right)^2\right]$$
$$\dots (9)$$

$$u\frac{\partial C}{\partial x} + v\frac{\partial C}{\partial y} = D_B\frac{\partial^2 C}{\partial y^2} + \frac{D_T}{T_\infty}\frac{\partial^2 T}{\partial y^2} \qquad \dots (10)$$

where u and v are the velocity components in the x and $y-$directions respectively; $= k/(\ c)_f$; and $= (\ c)_p/(\ c)_f$.

The associated boundary conditions are

$$u = u_w(x) = ax^m,\ v = 0,\ T = T_w,\ C = C_w \ \text{ at } \ y = 0$$

$$u \to u_\infty(x) = bx^m,\ v \to 0,\ T \to T_\infty,\ C \to C_\infty \ \text{ as } \ y \to \infty$$
$$\dots (11)$$

According to the modified Bernoulli's equation for the steady MHD flow, the pressure gradient in the $x-$direction[20] is:

$$u_\infty \frac{du_\infty}{dx} = -\frac{1}{\rho_f}\frac{\partial p}{\partial x} - \frac{B^2(x)}{\rho_f}u_\infty \qquad \ldots (12)$$

Eliminating $\partial p/\partial x$ between Eqs (8) and (12) gives

$$u\frac{\partial u}{\partial x} + v\frac{\partial u}{\partial y} = u_\infty\frac{du_\infty}{dx} + \frac{\mu}{\rho_f}\frac{\partial^2 u}{\partial y^2} + \frac{B^2(x)}{\rho_f}(u_\infty - u)\cdots (13)$$

The stream function $\psi = \psi(x,y)$ is introduced for which the velocity components u and v are defined as

$$u = \frac{\partial \psi}{\partial y},\ v = -\frac{\partial \psi}{\partial x}, \text{where continuity Eq. (7) is}$$

satisfied identically. Further, the similarity transformations are defined as[26]:

$$\psi = \sqrt{\frac{2\,ax^{m+1}}{m+1}}\,f(\eta),\quad \theta(\eta) = \frac{T-T_\infty}{T_w - T_\infty}$$

$$\phi(\eta) = \frac{C-C_\infty}{C_w - C_\infty},\quad \eta = y\sqrt{\frac{(m+1)ax^{m-1}}{2}}$$

$$\ldots (14)$$

Substituting Eq. (14) into Eqs (9), (10) and (13), the coupled system of nonlinear ordinary differential equations is:

$$f''' + ff'' - \left(\frac{2m}{m+1}\right)f'^2 + \left(\frac{2m}{m+1}\right)\varepsilon^2 - \left(\frac{2}{m+1}\right)M(f'-\varepsilon) = 0 \qquad \ldots (15)$$

$$\Pr_N \theta'' + f\theta' + Nb\,\theta'\phi' + Nt\,\theta'^2 = 0 \qquad \ldots (16)$$

$$\phi'' + Le\,f\phi' + \frac{Nt}{Nb}\theta'' = 0 \qquad \ldots (17)$$

where $\Pr_N = \frac{1}{\Pr}(1+\frac{4}{3}N);\ \Pr = \frac{\nu}{\alpha},$ the Prandtl number;

and $N = \frac{4\,{}^*T_\infty^3}{k^*},$ the radiation parameter and

$$M = \frac{B_0^2}{a\rho_f},\ \varepsilon = \frac{b}{a},\ Le = \frac{\alpha}{D_B},\ \alpha = \frac{k}{\rho c_f} \qquad \ldots (18)$$

$$Nb = \frac{D_B(C_w - C_\infty)}{\nu},\ Nt = \frac{D_T(T_w - T_\infty)}{T_\infty \nu}$$

where M is the magnetic parameter called Hartmann number; ε, the velocity ratio parameter; Le, the Lewis

number; ν, the kinematic viscosity of the fluid; Nb the Brownian motion parameter; and Nt the thermophoresis parameter. Here the magnetic field strength B should be proportional to x to the power $(m–1)/2$ in order to eliminate the dependence of M on x, i.e. $B(x) = B_0 x^{(m-1)/2}$ where B_0 is the uniform magnetic field strength[26].

The corresponding boundary conditions are transformed to

$$f(\eta) = 0,\ f'(\eta) = 1,\ \theta(\eta) = 1,\ \phi(\eta) = 1 \quad \text{at}\quad \eta = 0$$

$$f'(\eta) \to \varepsilon,\ \theta(\eta) \to 0,\ \phi(\eta) \to 0 \quad \text{as}\quad \eta \to \infty$$

$$\ldots (19)$$

The quantities of practical interest in velocity, heat and mass transfer characteristics for the nanofluid motions are expressed in terms of the dimensionless parameters, such as skin-friction, C_f Nusselt number Nu and Sherwood number Sh, as defined below:

$$C_f = \frac{\tau_w}{\frac{1}{2}\rho u_w^2},\ Nu = \frac{q_w x}{k(T_w - T_\infty)},\ Sh = \frac{q_m x}{D_B(C_w - C_\infty)}$$

$$\ldots (20)$$

where $\tau_w = \mu(\partial u/\partial y)_{y=0}$, $q_w = -\left[k + \frac{4\,{}^*T_\infty^3}{3k^*}\right](\partial T/\partial y)_{y=0}$, and $q_m = -D_B(\partial C/\partial y)_{y=0}$; these are the shear stress (τ_w), heat flux (q_w) and mass flux (q_m) at the surface respectively. Using variables [Eq. (14)], the associated expressions for dimensionless skin-friction coefficient $C_{fx}(0) = f''(0)$, reduced Nusselt number $-\theta'(0)$ and reduced Sherwood number $-\phi'(0)$ are defined as

$$C_{fx}(0) = \frac{C_f}{2}\sqrt{\frac{2}{m+1}\mathrm{Re_x}},\ -\theta'(0) = \frac{Nu}{\left(1+\frac{4}{3}N\right)\sqrt{\mathrm{Re_x}(m+1)/2}},$$

$$-\phi'(0) = \frac{Sh}{\sqrt{\mathrm{Re_x}(m+1)/2}}$$

$$\ldots (21)$$

where $\mathrm{Re}_x = u_w(x)x/\nu$ is the local Reynolds number based on the stretching velocity. The transformed nonlinear ordinary differential Eqs (15)-(17) subjected to boundary conditions [Eq. 19] are solved numerically by means of Keller-box method[27-30].

Results and Discussion

The magnetohydrodynamic (MHD) and radiation effects on the stagnation-point flow of nanofluid towards a nonlinear stretching sheet are investigated

theoretically. The transformed nonlinear ordinary differential equations [Eqs (15)-(17)] subjected to boundary conditions [Eq. (19)] are numerically solved using the Keller-box method. Results for some physical parameters of interest such as Hartmann number (M), velocity ratio parameter (ε), radiation parameter (N), Prandtl number (Pr), Lewis number (Le), Brownian motion parameter (Nb) and thermophoresis parameter (Nt) for the velocity, temperature and concentration profiles as well as for the skin-friction coefficient, the reduced Nusselt and Sherwood numbers are reported. Table 1 shows a comparison of our results for reduced Nusselt number $-\theta'(0)$ and reduced Sherwood number $-\phi'(0)$ by taking the Hartmann number (M), radiation parameter (N) and the velocity ratio parameter (ε) equal to zero and the power law velocity parameter $m = 1$, with those obtained by Khan and Pop[6] and the findings are found to be in a good agreement.

The variations of reduced Nusselt number $-\theta'(0)$, reduced Sherwood number $-\phi'(0)$ and skin-friction coefficient $C_{fx}(0)$ for different values of Nb, Nt, Pr, Le, M, N, ε and m are shown in Table 2. It is observed that $-\theta'(0)$ decreases with the increasing values of Nb, Nt, N and Le while it increases with the increasing values of Pr and ε. The large values of Brownian motion parameter impacts a large extent of the fluid and results in thickening of the thermal boundary layer. Also, the increasing values of thermophoresis parameter results in a deeper penetration into the fluid and causes the thermal boundary layer to be thicker. However, it is found that $-\phi'(0)$ decreases for the increasing values of Nt and Pr, whereas increases for the increasing values of Nb, Le, N and ε. Further, it is also observed that $C_{fx}(0)$ decreases for the increasing values of ε. Physically, it is true that positive values of skin-friction coefficient for the case when $\varepsilon < 1$ means

that the fluid exerts a drag force on the solid boundary and vice versa for the negative values of skin-friction coefficient when $\varepsilon > 1$[31]. Furthermore, it is noted that for the increasing values of M and m, the values of $-\theta'(0)$ and $-\phi'(0)$ decrease when $\varepsilon < 1$, whereas increase when $\varepsilon > 1$ and $C_{fx}(0)$ increases when $\varepsilon < 1$ while decreases when $\varepsilon > 1$.

Graphical results for different flow parameters are shown in Figs 2 - 4. The effects of M and m on the velocity profile $f'(\ )$ for the fixed values of Nb, Nt, N, Pr and Le for both cases of $\varepsilon < 1$ and $\varepsilon > 1$ are shown in Fig. 2. It is evident from this figure that for the case when $\varepsilon < 1$, $f'(\ )$ decreases for the increasing values of M and m, whereas it increases for the increasing values of M and m when $\varepsilon > 1$. It is

Table 2–Variations in reduced Nusselt number $-\theta'(0)$, the reduced Sherwood number $-\phi'(0)$ and skin-friction coefficient $C_{fx}(0)$

Nb	Nt	Pr	Le	M	N	ε	m	$-\theta'(0)$	$-\phi'(0)$	$C_{fx}(0)$
0.1	0.1	1.0	10	0.1	1.0	0.1	0.5	0.3273	2.2490	0.9161
0.5	0.1	1.0	10	0.1	1.0	0.1	0.5	0.2801	2.3165	0.9161
0.1	0.5	1.0	10	0.1	1.0	0.1	0.5	0.3019	1.9989	0.9161
0.1	0.1	7.0	10	0.1	1.0	0.1	0.5	0.8442	2.0837	0.9161
0.1	0.1	1.0	25	0.1	1.0	0.1	0.5	0.3267	3.7444	0.9161
0.1	0.1	1.0	10	2.5	1.0	0.1	0.5	0.2651	2.2143	1.8490
0.1	0.1	1.0	10	2.5	1.0	1.1	0.5	0.5202	2.5005	-0.2302
0.1	0.1	1.0	10	0.1	3.0	0.1	0.5	0.2093	2.2858	0.9161
0.1	0.1	1.0	10	0.1	1.0	0.6	0.5	0.4299	2.3519	0.5041
0.1	0.1	1.0	10	0.1	1.0	1.1	0.5	0.5073	2.4781	-0.1460
0.1	0.1	1.0	10	0.1	1.0	2.0	0.5	0.6207	2.7167	-1.7629
0.1	0.1	1.0	10	0.1	1.0	0.1	5.0	0.3115	2.2038	1.1775
0.1	0.1	1.0	10	0.1	1.0	1.1	5.0	0.5089	2.4851	-0.2034

Table 1—Comparison of the reduced Nusselt number $-\theta'(0)$ and the reduced Sherwood number $-\phi'(0)$ when $M = N = \varepsilon = 0$, Pr = $Le = 10$ and $m = 1$

Nb	Nt	Khan and Pop[6]		Present Results	
		$-\theta'(0)$	$-\phi'(0)$	$-\theta'(0)$	$-\phi'(0)$
0.1	0.1	0.9524	2.1294	0.9524	2.1294
0.2	0.2	0.3654	2.5152	0.3654	2.5152
0.3	0.3	0.1355	2.6088	0.1355	2.6088
0.4	0.4	0.0495	2.6038	0.0495	2.6038
0.5	0.5	0.0179	2.5731	0.0179	2.5731

Curve	Nb	Nt	N	Le	Pr	M	ε	m
I	0.1	0.1	1.0	10	1.0	0.1	1.9	0.5
II	0.1	0.1	1.0	10	1.0	0.1	1.9	0.5
III	0.1	0.1	1.0	10	1.0	**1.0**	1.9	0.5
IV	0.1	0.1	1.0	10	1.0	0.1	**2.0**	0.5
V	0.1	0.1	1.0	10	1.0	0.1	1.9	**5.0**

Curve	Nb	Nt	N	Le	Pr	M	ε	m
VI	0.1	0.1	1.0	10	1.0	0.1	0.1	0.5
VII	0.1	0.1	1.0	10	1.0	**1.0**	0.1	0.5
VIII	0.1	0.1	1.0	10	1.0	0.1	**0.2**	0.5
IX	0.1	0.1	1.0	10	1.0	0.1	0.1	**5.0**
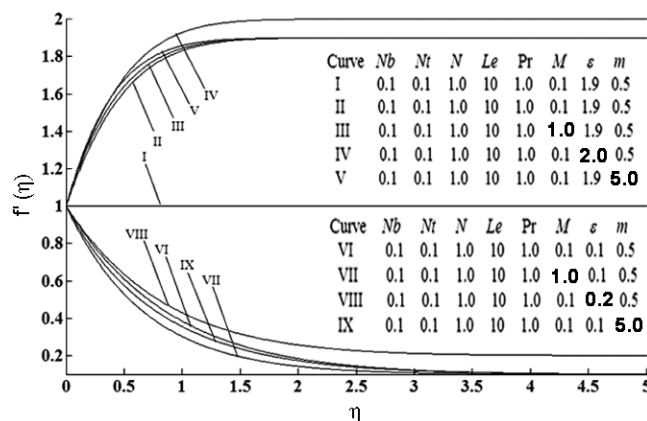
Fig. 2–Variation in velocity profiles $f'(\ )$ with η for different values of M, ε and m

also observed that $f'(\ )$ increases for increasing values of ε in both cases ($\varepsilon > 1$ and $\varepsilon > 1$) Physically, this is true because of the reason that increasing values of Hartmann number (M) increase the resistive forces on the sheet which reduce the fluid velocity and hence the motion of the fluid becomes slow. Further, it is noted that for the increasing values of different flow parameters, $f'(\ )$ coincides with each other when $\varepsilon = 1$. This means that in the case when the external stream velocity becomes equal to the stretching velocity, the flow field is not influenced by the different values of the incorporated parameters. This implies that the fluid and surface velocities are same. It is interesting to note that for the case of $\varepsilon > 1$ i.e. when the external stream velocity increases as compared to the stretching velocity, momentum boundary layer thickness becomes shorten in comparison to the case when $\varepsilon < 1$ and causes inverted boundary layer structure. Moreover, for the case $\varepsilon = 1$, $f'(\ )$ coincides with each other and results in a degenerate inviscid flow where the stretching matches the conditions at infinity[32]. This means that in the case when the external stream velocity becomes equal to the stretching velocity, the flow field is not influenced by the different values of the incorporated flow parameters.

Figures 3(a) and (b) present the temperature profiles (η) for the combined effects of Nb, Nt, Pr, M, N, ε and m for the both cases of $\varepsilon < 1$ and $\varepsilon > 1$ when $Le = 10$. It is observed that (η) decreases for the increasing values of Pr and ε, whereas it increases for the increasing values of Nb, Nt and N. Physically, this behavior is meaningful due to the fact that it depends upon the formation of nanofluid which is a combination of the base fluid (water and ethylene glycol) and nanoparticles (Cu, aluminium, titanium). With increasing the viscosity of the base fluid, the thermal boundary layer thickness decreases and the heat transfer is found to be smaller for large values of Pr. It shows that the suspended nanoparticles motions are more affected by the highly viscous fluids and results for less colloidal forces among each other. Further, Figs 3(a) and (3b) indicate that (η) increases for the increasing values of M and m when $\varepsilon < 1$, whereas it decreases for the increasing values of
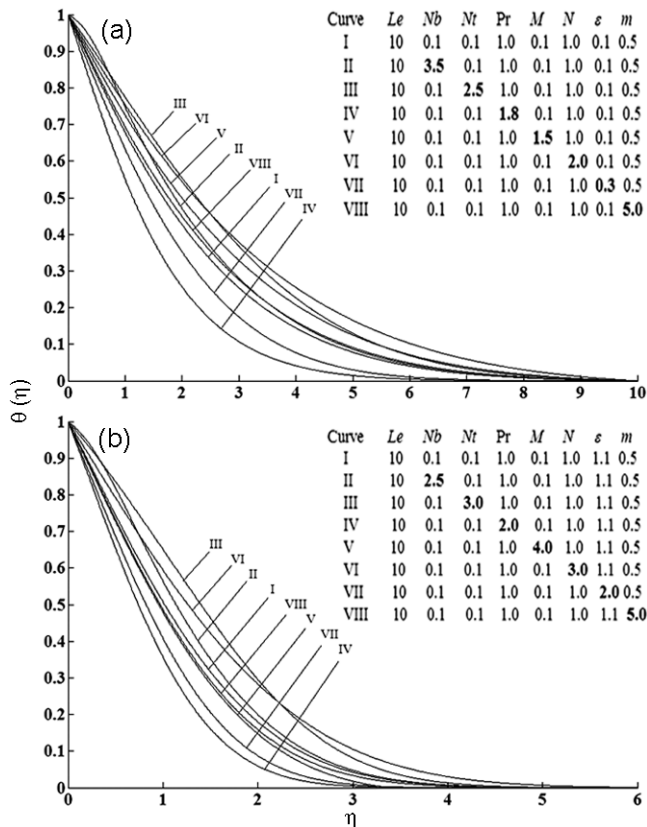

Curve	Le	Nb	Nt	Pr	M	N	ε	m
I	10	0.1	0.1	1.0	0.1	1.0	0.1	0.5
II	10	3.5	0.1	1.0	0.1	1.0	0.1	0.5
III	10	0.1	2.5	1.0	0.1	1.0	0.1	0.5
IV	10	0.1	0.1	1.8	0.1	1.0	0.1	0.5
V	10	0.1	0.1	1.0	1.5	1.0	0.1	0.5
VI	10	0.1	0.1	1.0	0.1	2.0	0.1	0.5
VII	10	0.1	0.1	1.0	0.1	1.0	0.3	0.5
VIII	10	0.1	0.1	1.0	0.1	1.0	0.1	5.0

Curve	Le	Nb	Nt	Pr	M	N	ε	m
I	10	0.1	0.1	1.0	0.1	1.0	1.1	0.5
II	10	2.5	0.1	1.0	0.1	1.0	1.1	0.5
III	10	0.1	3.0	1.0	0.1	1.0	1.1	0.5
IV	10	0.1	0.1	2.0	0.1	1.0	1.1	0.5
V	10	0.1	0.1	1.0	4.0	1.0	1.1	0.5
VI	10	0.1	0.1	1.0	0.1	3.0	1.1	0.5
VII	10	0.1	0.1	1.0	0.1	1.0	2.0	0.5
VIII	10	0.1	0.1	1.0	0.1	1.0	1.1	5.0

Fig. 3–Variation in temperature profiles (η) with η for different values of Nb, Nt, Pr, M, N and m when (a) $\varepsilon < 1$ and (b) $\varepsilon > 1$

Curve	Nb	Nt	Pr	Le	M	N	ε	m
I	0.1	0.1	1.0	10	0.1	1.0	0.1	0.5
II	0.5	0.1	1.0	10	0.1	1.0	0.1	0.5
III	0.1	0.2	1.0	10	0.1	1.0	0.1	0.5
IV	0.1	0.1	4.0	10	0.1	1.0	0.1	0.5
V	0.1	0.1	1.0	20	0.1	1.0	0.1	0.5
VI	0.1	0.1	1.0	10	2.5	1.0	0.1	0.5
VII	0.1	0.1	1.0	10	0.1	3.0	0.1	0.5
VIII	0.1	0.1	1.0	10	0.1	1.0	0.6	0.5
IX	0.1	0.1	1.0	10	0.1	1.0	0.1	5.0

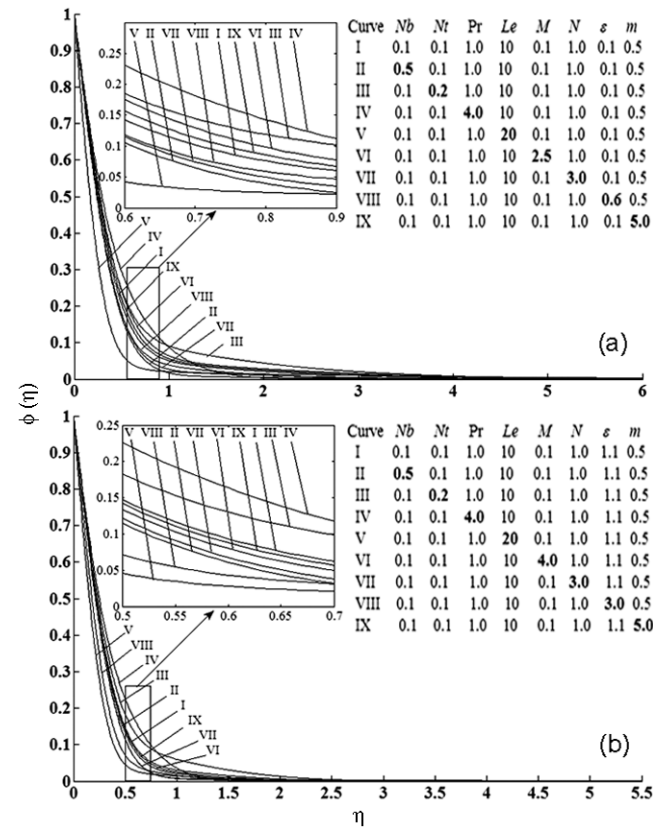| Curve	Nb	Nt	Pr	Le	M	N	ε	m
I	0.1	0.1	1.0	10	0.1	1.0	1.1	0.5
II	0.5	0.1	1.0	10	0.1	1.0	1.1	0.5
III	0.1	0.2	1.0	10	0.1	1.0	1.1	0.5
IV	0.1	0.1	4.0	10	0.1	1.0	1.1	0.5
V	0.1	0.1	1.0	20	0.1	1.0	1.1	0.5
VI	0.1	0.1	1.0	10	4.0	1.0	1.1	0.5
VII	0.1	0.1	1.0	10	0.1	3.0	1.1	0.5
VIII	0.1	0.1	1.0	10	0.1	1.0	3.0	0.5
IX	0.1	0.1	1.0	10	0.1	1.0	1.1	5.0

Fig. 4–Variation in concentration profiles (η) with η for different values of Nb, Nt, Pr, Le, M, N and m when (a) $\varepsilon < 1$ and (b) $\varepsilon > 1$

M and m when > 1. These figures show that for < 1, the thermal boundary layer thickness is greater compared to the case when > 1.

The concentration profiles (η) are shown in Fig. 4 for different values of embedded flow parameters in both cases of $\varepsilon < 1$ and $\varepsilon < 1$. It is observed from Fig. 4(a) that (η) decreases for the increasing values of Nb, N, Le and ε, whereas it increases for the increasing values of Nt, Pr, M and m. The large values of Le play an important role in shortening the concentration boundary layer for the mass fraction. Figure 4(b) depicts that for the dominated free stream velocity, (η) increases for increasing values of Nb and Pr, whereas it decreases for the increasing values of Nt, M, N, Le, ε and m. These figures show that concentration boundary layer thickness is greater for < 1 as compared to that for > 1. Since all the profiles discussed above descend smoothly in the free stream satisfying the boundary conditions, this ensures the accuracy of the obtained numerical results.

Conclusion

For the accuracy purpose, present results are compared with those obtained by Khan and Pop[6] and found in a good agreement. The point wise conclusion of the presented study is given as follows:

- The reduced Nusselt number and the reduced Sherwood number decrease for the increasing values of M and m, whereas skin-friction coefficient increases when < 1 but opposite effects are observed for the case when > 1.
- The increasing values of Nt and N show that the reduced Nusselt number decreases, whereas the reduced Sherwood number is found in opposite behavior.
- The magnitude of the skin-friction coefficient $C_{fx}(0)$ is zero for $= 1$.
- Velocity profiles are observed in opposite manner for the increasing values of M and m when < 1 and > 1 but these profiles are increased for the increasing values of $.$
- The momentum, thermal and concentration boundary layers are found shortened when free stream velocity is greater than stretching velocity.

Acknowledgement

References
1   Sahoo B, *Comm Nonlinear Sci Numer Simul*, 15 (2010) 602.
2   Fetecau C, Hayat T & Fetecau C, *Int J Nonlinear Mech*, 41 (2006) 880.
3   Fetecau C, Fetecau C, Kamran M & Vieru D, *J Non-Newtonian Fluid Mech*, 156 (2009) 189.
4   Kuznetsov A V & Nield D A, *Int J Therm Sci*, 49 (2010) 243.
5   Bachok N, Ishak A & Pop I, *Int J Therm Sci*, 49 (2010) 1663.
6   Khan W A & Pop I, *Int J Heat Mass Transf*, 53 (2010) 2477.
7   Choi S U S, *American Society of Mechanical Engineers, Fluids Engineering Division, San Francisco, Calif, USA*, 231 (1995) 99.
8   Eastman J A, Choi S U S, Li S, Yu W & Thompson L J, *Appl Phys Lett*, 78 (2001) 718.
9   Choi S U S, Zhang Z G, Yu W, Lockwood F E & Grulke E A, *Appl Phys Lett*, 79 (2001) 2252.
10 Masuda H, Ebata A, Teramae K & Hishinuma N, *Netsu Bussei*, 7 (1993) 227.
11 Labropulu F, Li D & Pop I, *Int J Therm Sci*, 49 (2010) 1042.
12 Hiemenz K, *Dingler's Polytech J*, 326 (1911) 321.
13 Nazar R, Amin N, Filip D & Pop I, *Int J Nonlinear Mech*, 39 (2004) 1227.
14 Lok Y Y, Amin N & Pop I, *Int J Nonlinear Mech*, 41(2006) 622.
15 Mahapatra T R & Gupta A S, *Heat Mass Transf*, 38 (2002) 517.
16 Mustafa M, Hayat T, Pop I, Asghar S & Obaidat S, *Int J Heat Mass Transf*, 54 (2011) 5588.
17 Hamad M A A & Ferdows M, *Commun Nonlinear Sci Numer Simul*, 17 (2012) 132.
18 Alsaedi A, Awais M & Hayat T, *Commun Nonlinear Sci Numer Simul*, 17 (2012) 4210.
19 Nadeem S, Rehman A, Vajravelu K, Lee J & Lee C, *Math Prob Eng*, 2012 (2012) Article ID 378259, doi:10.1155/2012/378259.
20 Jafar K, Ishak A & Nazar R, *J Aerosp Eng*, 26 (2011) 829.
21 Hayat T, Javed T & Abbas Z, *Nonlinear Analy Real World Appl*, 10 (2009) 1514.
22 Mahapatra T R & Gupta A S, *Acta Mech*, 152 (2001) 191.
23 Rana P & Bhargava R, *Commun Nonlinear Sci Numer Simul*, 17 (2012) 212.
24 Cess R D, *Int J Heat Mass Transf*, 9 (1966) 1269.
25 Hady F M, Ibrahim F S, Abdel-Gaied S M & Eid M R, *Nanoscale Res Lett*, 7 (2012) 1.
26 Afify A A, *Commun Nonlinear Sci Numer Simul*, 14 (2009) 2202.
27 Cebeci T & Bradshaw P, *Momentum Transfer in Boundary Layers*, (Hemisphere Publishing Corporation, New York) 1977.
28 Cebeci T & Bradshaw P, *Physical and Computational Aspects of Convective Heat Transfer* (Springer-Verla, New York) 1988.
29 Salleh M Z, Nazar R & Pop I, *Meccanica*, 47 (2012) 1261.
30 Imran Anwar, Sharidan Shafie & Mohd Zuki Salleh, *Walailak J Sci Tech*, 11 (2014) 569.
31 Bachok N, Ishak A & Pop I, *Nanoscale Res Lett*, 6 (2011) 623.
32 Ishak A, Jafar K, Nazar R & Pop I, *Physica A*, 388 (2009) 3377